

# LEARNING ACTIVATION FUNCTIONS WITH PCA ON A SET OF DIVERSE PIECEWISE-LINEAR SELF-TRAINED MAPPINGS

**Anonymous authors**

Paper under double-blind review

## ABSTRACT

This work explores a novel approach to learning activation functions, moving beyond the current reliance on human-engineered designs like the ReLU. Activation functions are crucial for the performance of deep neural networks, yet selecting an optimal one remains challenging. While recent efforts have focused on automatically searching for these functions using a parametric approach, our research does not assume any predefined functional form and lets the activation function be approximated by a subnetwork within a larger network, following the Network in Network (NIN) paradigm. We propose to train several networks on a range of problems to generate a diverse set of effective activation functions, and subsequently apply Principal Component Analysis (PCA) to this collection of functions to uncover their underlying structure. Our experiments show that only a few principal components are enough to explain most of the variance in the learned functions, and that these components have in general a simple, identifiable analytical form. Experiments using the analytical function form achieve state of the art performance, highlighting the potential of this data-driven approach to activation function design.

## 1 INTRODUCTION

Deep learning, a powerful branch of machine learning, is the backbone of modern artificial intelligence. It has achieved remarkable success in various domains, from computer vision to drug discovery and autonomous vehicles, by learning intricate patterns and representations from massive datasets. This capability stems from the architecture of deep neural networks (DNNs), which are built with multiple layers of interconnected nodes. At the root of each of these nodes lies a crucial component: the activation function.

Activation functions introduce non-linearity into a neural network, which is essential for solving complex, real-world problems. Without them, a neural network would simply be a linear model. To provide a foundational basis for our work, we first review the essential properties and historical context of these functions. The two most critical requirements are non-linearity and differentiability. The primary and most indispensable purpose of an activation function, denoted as  $\sigma$ , is to introduce non-linearity. This fundamental requirement is formally justified by the Universal Approximation Theorem. Pioneering work by Cybenko (Cybenko, 1989) and Hornik (Hornik et al., 1989; Hornik, 1991) established that a feed-forward network with a single hidden layer can approximate any continuous function to a desired degree of precision, provided the activation function is non-linear. The mere existence of a non-linear function is a sufficient condition to allow for powerful function approximation. Beyond non-linearity, differentiability is a crucial property that enables gradient-based optimization. The standard backpropagation algorithm (Rumelhart et al., 1986) updates network weights by computing the gradient of the loss function via the chain rule. The activation function must therefore have a well-defined derivative to act as a backwards-traversable link in the network’s computational graph. While strict differentiability is ideal, piecewise differentiability is sufficient in practice. Furthermore, the smoothness of an activation function, related to its higher-order differentiability, can significantly impact training dynamics by producing a smoother loss landscape, which is generally easier for optimization algorithms to navigate (Santurkar et al., 2018; Misra, 2019).

054 The history of activation functions reflects the evolution of deep learning itself. Early networks  
055 like the Perceptron (Rosenblatt, 1958) used a simple step function, which was non-differentiable  
056 and thus incompatible with gradient-based learning. With the popularization of the backpropagation  
057 algorithm (Rumelhart et al., 1986; Linnainmaa, 1976; Werbos, 2005), smooth and differentiable  
058 functions like the sigmoid and tanh became the standard. However, their saturating nature led to  
059 the *vanishing gradient* problem, which severely hampered the training of very deep networks. The  
060 Rectified Linear Unit (ReLU) (Nair & Hinton, 2010) solved this problem for positive activations  
061 and was computationally inexpensive, becoming a key factor in the early successes of deep learn-  
062 ing. Since then, numerous variants have been proposed to address ReLU’s *dying neuron* problem,  
063 such as Leaky ReLU (LReLU) (Maas et al., 2013), which introduced a small non-zero slope to the  
064 negative part of the function. This trend led to Parametric ReLU (PReLU) (He et al., 2015), which  
065 generalized LReLU by making the slope a learnable parameter. More recently, functions like Swish  
066 (Ramachandran et al., 2017) and Mish (Misra, 2019) have demonstrated that non-monotonicity can  
067 enhance model expressivity and improve gradient flow. A crucial aspect of these functions, which  
068 were discovered using automated search techniques, is that they empirically outperform other func-  
069 tions, showing that there could be better options than those designed by humans. The computa-  
070 tional cost of activation functions is also a critical practical concern, as simple functions relying  
071 on inexpensive hardware operations (e.g., ReLU) are significantly faster than those involving costly  
operations like exponentials (e.g., Sigmoid, Tanh) (Datta, 2020).

072 A notable trend in recent years has been to move away from manually designed functions toward  
073 learnable activation functions, whose shapes are optimized during training. This evolution mirrors  
074 a broader trend in machine learning, reflecting a shift from manual engineering to automated dis-  
075 covery. The central motivation of this work is to formulate and study the behavior of an adaptive  
076 activation function whose parameters are learned dynamically during a neural network’s training  
077 process. While traditional, static functions like ReLU and sigmoid have driven significant progress,  
078 they operate under a fundamental limitation: their form is fixed before training begins. This static  
079 nature can hinder the network’s ability to capture complex, non-linear relationships and may lead to  
080 issues like vanishing gradients or slow convergence. To address these shortcomings, several strate-  
081 gies have been proposed. One approach extends existing functions with learnable parameters, as  
082 seen in PReLU (He et al., 2015) and the original trainable version of Swish (Ramachandran et al.,  
083 2017). Another method uses a linear combination of basis functions to construct a more complex,  
084 adaptable shape, a technique used in Adaptive Piecewise Linear (APL) Units (Agostinelli et al.,  
085 2014) and kernel-based approaches (Scardapane et al., 2019). A third line of research has focused  
086 on redesigning the network’s internal components to create implicitly learned activation mecha-  
087 nisms. This includes the Network in Network (NIN) architecture (Lin et al., 2013), where a small  
088 multi-layer perceptron (MLP) replaces the standard activation, and Maxout networks (Goodfellow  
et al., 2013), which learn a piecewise linear activation.

089 Motivated by this trend, we propose a new approach by exploring the concept of a Self-Learning  
090 Activation Function (SLAF). Unlike parametric search methods that assume a predefined functional  
091 form, we model the SLAF as a small neural network—specifically, a single-layer MLP. This ap-  
092 proach, which closely resembles the one presented in NIN (Lin et al., 2013) and the APL units in  
093 (Agostinelli et al., 2014), allows the network to learn the optimal non-linearity in a less biased way,  
094 as the function’s parameters are learned and adjusted dynamically alongside the network’s weights  
095 and biases using backpropagation. However, the main contribution of this work is not the SLAF  
096 itself, but a novel, straightforward method for discovering new activation functions from several  
097 SLAFs trained on a variety of problems. We do not perform any parametric search like in similar  
098 approaches (Ramachandran et al., 2017). Instead, we train a diverse collection of networks to learn a  
099 wide variety of SLAF instances. We then perform a Principal Component Analysis (PCA) on these  
100 learned functions to identify their main functional modes. By fitting simple analytical functions to  
101 these principal components, we are able to derive a new, powerful activation function, which we term  
102 *twish*. This approach simplifies the search process and provides a more generalizable method for  
103 discovering functional activation functions. Our results demonstrate that the *twish* function, which is  
104 a generalization of the Swish, consistently outperforms other popular activations and leads to faster  
105 convergence, particularly on more complex datasets. Our findings demonstrate that a data-driven  
106 approach to function discovery provides a powerful foundation for developing more sophisticated  
and robust activation functions for neural networks.

107

## 2 LEARNING THE BASE ACTIVATION FUNCTIONS

In this section, we first define the form of our activation function as a small network within the main network, and then we detail the procedure that is followed to obtain a diverse collection of basic activation functions. This set of activations will be the basis for the subsequent principal component analysis.

### 2.1 SLAF DEFINITION

The core of this research is a small feedforward network that implements a self-learnable activation function (SLAF). Because activation functions are pointwise operations, the SLAF is designed to take a single scalar input and produce a single scalar output. The SLAF is structured as a one-hidden-layer network that maps its scalar input to a higher-dimensional latent space before collapsing it back into a single output value. More specifically, the SLAF’s single scalar input is transformed by a dense linear layer that maps it to  $N$  hidden units, using weights  $W_1 \in \mathbb{R}^{1 \times N}$  and bias  $b_1 \in \mathbb{R}^N$ . A ReLU activation function is then applied, and an output dense layer maps the  $N$  hidden units back to a single output value, with weights  $W_2 \in \mathbb{R}^{N \times 1}$  and bias  $b_2 \in \mathbb{R}$ . Figure 1 provides a visual representation of the SLAF for  $N = 2, 4, 8$ .

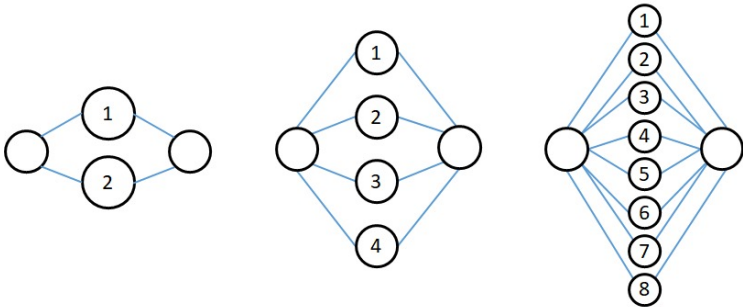


Figure 1: A diagram of SLAF-2, SLAF-4 and SLAF-8.

This definition can be understood as a piecewise linear function with as many pieces as hidden units. The intuition is that the final unit is a weighted sum of a finite number of ReLU-like functions. In the end the expression is

$$f(x) = \sum_i W_{2i} \text{ReLU}(W_{1i}x + b_{1i}) + b_2. \quad (1)$$

This is very similar to the piecewise linear function definition of the APL activation function in Agostinelli et al. (2014).

### 2.2 TRAINING

The parameters of the SLAF are trained jointly with those of the main network in which it is embedded. Our initial experiments use feed-forward neural networks trained on the MNIST, Fashion-MNIST, and CIFAR-10 datasets. The networks consist of two densely connected layers. They first reduce the input dimensions from  $H \times W \times C$  to a 64-dimensional hidden state before finally generating a 10-dimensional vector of logits for classification. Given the varying input shapes ( $28 \times 28 \times 1$  for MNIST and FashionMNIST, and  $32 \times 32 \times 3$  for CIFAR-10), the networks have approximately 51K trainable parameters for MNIST-like images and 66K for CIFAR-10 images.

For each dataset and for each number of SLAF units,  $N \in \{2, 4, 8, 16, 32, 64\}$ , we trained 256 different networks. Each network was trained for a fixed number of 10 epochs using the Adam optimizer (Kingma & Ba, 2014) to minimize a cross-entropy loss between the output probabilities and the expected targets. To ensure comparable input scales, pre-activations were batch-normalized before applying the SLAF activations. A random sample of the learned activation functions for  $N = 16$  is shown in Figure 2. The  $y$ -axis scale varies for each plot to facilitate easier comparison of

the function shapes. We observe that the learned shapes are similar, though diverse, across different problems. This is also true for different values of  $N$  (not shown).

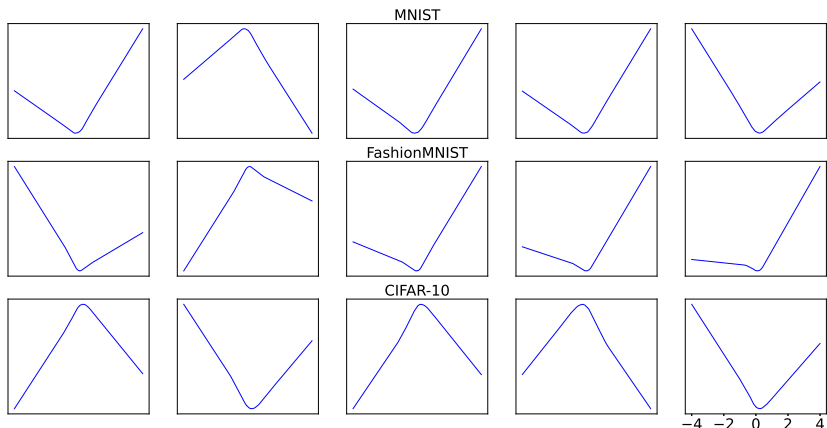


Figure 2: Sample SLAFs obtained for  $N = 16$  for the datasets MNIST (top), FashionMNIST (middle) and CIFAR-10 (bottom).

### 3 ACTIVATION FUNCTION DISCOVERY THROUGH PCA

The main idea of this work is to use the set of trained activation functions as the basis for a Principal Component Analysis (PCA) that allows to identify the main functional modes. Therefore, our next step is to perform PCA to identify the functional shapes that account for the most variance in the SLAF functions. For this analysis, we used all 4608 trained activation functions (3 datasets  $\times$  6 SLAF functions  $\times$  256 networks). To perform the PCA, each SLAF was evaluated at 1600 equally spaced points in the range  $[-4, 4]$ . The analysis yielded a series of eigenfunctions that represent the primary modes of variation in the function shapes. The first two principal components, which jointly explain more than 99.5% of the total variance, are shown in Figure 3. Interestingly, these two components can be approximated by simple analytical functions.

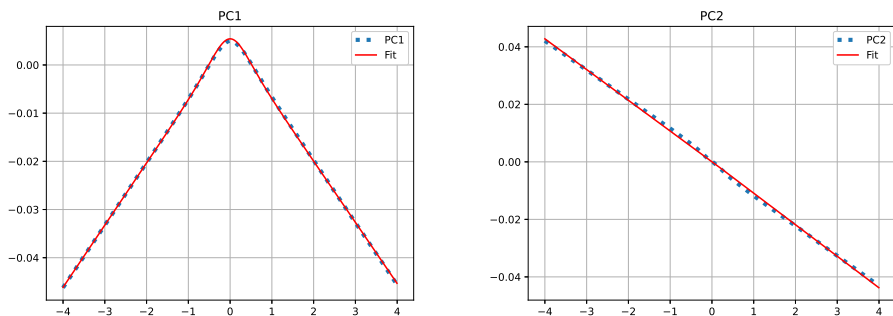


Figure 3: First two eigenfunctions obtained with PCA on the trained SLAFs.

The first principal component (PC1) is symmetric with respect to the  $y$ -axis, and consists of two linear branches with a smooth transition around  $x = 0$ . Up to a multiplicative constant, this shape can be understood as a soft absolute value function. Ignoring this scale factor and an additive bias, it can be formally approximated by

216  
217  
218  
219  
220  
221  
222  
223  
224  
225  
226  
227  
228  
229  
230  
231  
232  
233  
234  
235  
236  
237  
238  
239  
240  
241  
242  
243  
244  
245  
246  
247  
248  
249  
250  
251  
252  
253  
254  
255  
256  
257  
258  
259  
260  
261  
262  
263  
264  
265  
266  
267  
268  
269

$$f_1(x) = x \tanh(\beta x). \tag{2}$$

The original eigenfunction (blue, dotted) as well the approximation (red, solid), are shown in figure 3 (left panel). The second principal component (PC2), on the other hand, is essentially a linear function of  $x$  with no bias:

$$f_2(x) = \gamma x. \tag{3}$$

The right panel of figure 3 shows both the experimental eigenfunction (blue, dotted) and its analytical approximation (red, solid).

### 3.1 THE TWISH ACTIVATION FUNCTION

As previously noted, more than 99.5% of the variance in the shape of the SLAFs is explained with just the first two eigenfunctions. Even more, these two principal components can be well approximated by the expressions in equations 2 and 3. This suggests that the general functional shape of the learned activations can be characterized as a parametric function of the form:

$$f(x; \beta, \gamma) = x \tanh(\beta x) + \gamma x, \tag{4}$$

where  $\beta$  and  $\gamma$  are learnable parameters. It is interesting to note that, for  $\gamma = 1$ , the function resembles the Swish activation function (Ramachandran et al., 2017):

$$f(x; \beta, \gamma = 1) = 2x\sigma(2\beta x). \tag{5}$$

However, our learned function, which we term *twish*, generalizes this form. Unlike Swish, the *twish* function incorporates a wider variety of shapes for  $\gamma \neq 1$  (see figure 4), effectively having the Swish as a particular case. We named it *twish* because the functional form of its first principal component is similar to the Swish function, but uses a hyperbolic tangent instead of a sigmoid. In the following section, we describe additional experiments where we apply the *twish* function to the previous datasets using convolutional neural networks, comparing its performance against other state-of-the-art activations.

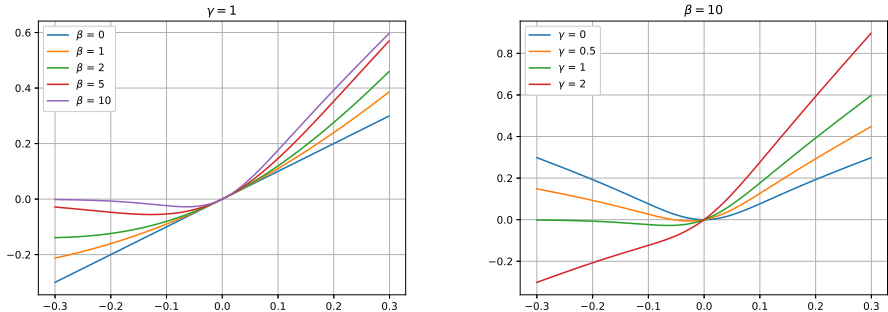


Figure 4: The twish function.

## 4 FURTHER EXPERIMENTS

To evaluate the potential benefits of the newly described *twish* activation function, we compare it with other commonly used functions: ReLU, pReLU, Swish, ELU, SELU, GELU and Mish. For this comparison, we use the same three datasets, namely MNIST, FashionMNIST, and CIFAR-10, with a custom convolutional neural network (CNN). In the case of the Swish and *twish* functions, the trainable parameters are shared across all the network’s neurons. The Swish  $\beta$  parameter is

270  
271  
272  
273  
274  
275  
276  
277  
278  
279  
280  
281

Table 1: Test accuracy at the end of the 30 training epochs.

AF	MNIST	FashionMNIST	CIFAR-10
relu	0.989 ± 0.001	0.905 ± 0.003	0.693 ± 0.008
prelu	0.989 ± 0.002	0.905 ± 0.004	0.702 ± 0.007
elu	0.987 ± 0.001	0.902 ± 0.003	0.679 ± 0.006
selu	0.986 ± 0.001	0.900 ± 0.004	0.662 ± 0.006
gelu	0.989 ± 0.002	0.904 ± 0.003	0.697 ± 0.007
mish	<b>0.990 ± 0.001</b>	0.903 ± 0.003	0.693 ± 0.006
swish	<b>0.990 ± 0.001</b>	0.905 ± 0.003	0.695 ± 0.006
twish	<b>0.990 ± 0.002</b>	<b>0.906 ± 0.004</b>	<b>0.705 ± 0.007</b>

282  
283  
284

285 initialized to 1, and the twish parameters are initially set so that the starting point is also a Swish  
286 with  $\beta = 1$ .

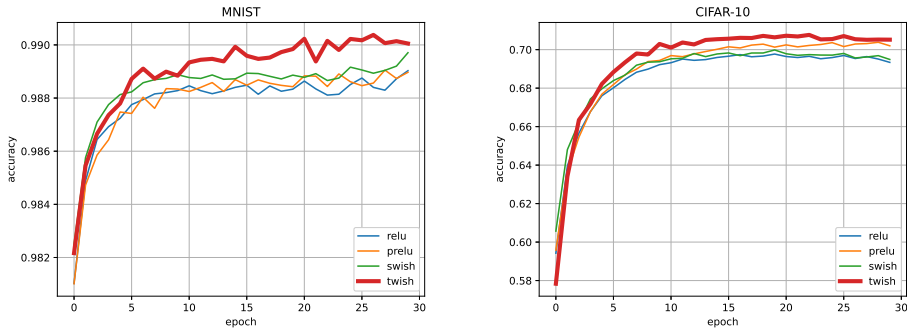
287  
288  
289  
290  
291  
292  
293  
294  
295  
296

The CNN has a simple architecture consisting of two convolutional layers with  $3 \times 3$  kernels, each followed by a max-pooling layer to halve the image resolution. The number of channels increases from 1 (for grayscale images) or 3 (for RGB images) to 16, and then to 32. After the two convolutional and pooling layers, the output is flattened before the final linear transformation to a 10-dimensional vector for classification. The size of this final fully connected layer differs between the datasets (MNIST/FashionMNIST vs. CIFAR-10) due to their varying initial image dimensions. The networks have approximately 20K and 25K trainable parameters for MNIST-like and CIFAR-10 images, respectively. As before, batch normalization is applied to all pre-activations. For each dataset and activation function, we train 64 networks for 30 epochs using the Adam optimizer (Kingma & Ba, 2014), and then average the results.

297  
298  
299  
300  
301  
302

Figure 5 shows the test set accuracy as a function of the training epoch for CNNs trained on MNIST (left panel) and CIFAR-10 (right panel). The curves represent the average accuracy over the 64 networks trained for each activation function. We observe that the twish function clearly dominates in both cases, outperforming the other activations by a wide margin throughout the entire training period. This superiority is consistent across both datasets, despite the overall difference in accuracy between the two problems. For a more detailed analysis, we refer the reader to Tables 1 and 2.

303  
304



315  
316  
317  
318

Figure 5: Test accuracy vs. training epoch for MNIST (left) and CIFAR-10 (right).

319  
320  
321  
322  
323

Table 1 displays the average test accuracy obtained after 30 training epochs for each of the three datasets. We observe that the twish function yields the best results in all cases. The performance difference is especially significant for the CIFAR-10 dataset, while the improvements on the simpler MNIST and FashionMNIST problems are less pronounced. For the simpler problems, the twish function likely implements a Swish-like solution. In contrast, for the more complex CIFAR-10 dataset, it appears to exploit its greater expressive power to outperform the other activation functions.

Table 2: Average number of epochs required to reach 90% of the total accuracy span achieved during the entire training process.

	AF	MNIST	FashionMNIST	CIFAR-10
relu		$9.5 \pm 4.0$	$4.5 \pm 1.2$	$8.0 \pm 1.7$
prelu		$9.7 \pm 5.0$	$5.1 \pm 1.3$	$7.5 \pm 1.7$
elu		$24.9 \pm 8.7$	$5.6 \pm 1.3$	$25.3 \pm 7.1$
selu		-	$6.5 \pm 1.8$	-
gelu		$7.8 \pm 3.8$	$4.5 \pm 1.1$	$7.1 \pm 1.3$
mish		$9.4 \pm 4.4$	$5.0 \pm 1.3$	$8.7 \pm 1.8$
swish		$7.0 \pm 3.0$	<b><math>4.4 \pm 1.0</math></b>	$7.2 \pm 1.5$
twish		<b><math>5.8 \pm 1.7</math></b>	$4.8 \pm 1.4$	<b><math>6.4 \pm 1.1</math></b>

Next, Table 2 analyzes the convergence time. We measure the average number of epochs required to reach 90% of the total accuracy span achieved during the entire training process<sup>1</sup>. Consistent with our previous results, the twish function generally shows faster convergence times. The only exception is FashionMNIST, where Swish reaches the convergence point slightly earlier. However, the differences among all four activations are not statistically significant for this dataset, with twish closely following Swish. Networks trained with the SELU activation function failed to reach the convergence point after 30 training epochs for the MNIST and CIFAR-10 problems.

Overall, our experiments demonstrate that the twish activation function consistently outperforms other popular activations like ReLU, pReLU, and Swish across several datasets. We have shown that twish not only achieves higher final accuracy, especially on the more complex CIFAR-10 dataset, but also leads to faster convergence during training. These results suggest that the enhanced expressive power of the twish function, derived from its learned parametric form, allows it to adapt more effectively to the complexities of different problems, offering a clear advantage over conventional activation functions.

## 5 CONCLUSIONS

This study has introduced a novel, data-driven methodology for discovering new activation functions, challenging the traditional reliance on manually designed functions or simple parametric searches. By modeling the activation function as a small neural network—a Self-Learning Activation Function (SLAF)—we were able to train a diverse collection of functional shapes. Our core contribution lies in this unique discovery process: using Principal Component Analysis (PCA) on these learned functions to identify their main functional modes. This approach allowed us to derive a new, powerful activation function, which we termed twish, by fitting simple analytical forms to the principal components. This methodology offers a more streamlined and less biased alternative to extensive parametric searches, simplifying the process of finding new and effective non-linearities for neural networks.

The experimental results presented here provide strong evidence for the effectiveness of the twish function. Our comparative analysis showed that twish consistently outperformed other widely-used activation functions, including ReLU, pReLU, and Swish, in terms of both final accuracy and convergence speed. This was particularly evident on the more complex CIFAR-10 dataset, where twish demonstrated a significant advantage. The superior performance of twish suggests that the expressive power of its learned form allows it to adapt more effectively to the complexities of a given problem, offering a clear advantage over conventional, fixed-form functions. The fact that twish generalizes the Swish function—which was itself the result of a complex automated search—highlights the strength and potential of our discovery method.

<sup>1</sup>The convergence point is defined as the epoch where the test accuracy first exceeds  $acc_{min} + 0.9(acc_{max} - acc_{min})$ , where  $acc_{min}$  and  $acc_{max}$  are the minimum and maximum accuracy values observed during training.

378 While our findings are promising, it is important to acknowledge the limitations of this initial study.  
 379 Our experiments were conducted on a restricted set of relatively small-scale datasets (MNIST, FashionMNIST, and CIFAR-10) and using simple feedforward and convolutional neural network architectures. Consequently, the results presented here are not directly comparable to the state-of-the-art performance on these benchmarks, which often rely on much deeper and more complex models.  
 380  
 381  
 382  
 383 The primary goal of this work was not to set new performance records, but rather to validate our novel method for activation function discovery and to introduce the twish function.  
 384

385 Despite these limitations, our work serves as a proof of concept for a new and promising approach to functional discovery in deep learning. We believe this methodology can be a valuable tool for future research. We encourage the broader scientific community to experiment with the twish function on a wider range of architectures and datasets. Further experimentation will be crucial to fully validate its effectiveness and to explore its potential in more advanced deep learning applications.  
 386  
 387  
 388  
 389  
 390

## 391 REFERENCES

- 392  
 393 Forest Agostinelli, Matthew Hoffman, Peter Sadowski, and Pierre Baldi. Learning activation functions to improve deep neural networks. *arXiv preprint arXiv:1412.6830*, 2014.  
 394  
 395 George Cybenko. Approximation by superpositions of a sigmoidal function. *Mathematics of control, signals and systems*, 2(4):303–314, 1989.  
 396  
 397 Leonid Datta. A survey on activation functions and their relation with xavier and he normal initialization. *arXiv preprint arXiv:2004.06632*, 2020.  
 398  
 399 Ian Goodfellow, David Warde-Farley, Mehdi Mirza, Aaron Courville, and Yoshua Bengio. Maxout networks. In *International conference on machine learning*, pp. 1319–1327. PMLR, 2013.  
 400  
 401 Kaiming He, Xiangyu Zhang, Shaoqing Ren, and Jian Sun. Delving deep into rectifiers: Surpassing human-level performance on imagenet classification. In *Proceedings of the IEEE international conference on computer vision*, pp. 1026–1034, 2015.  
 402  
 403 Kurt Hornik. Approximation capabilities of multilayer feedforward networks. *Neural networks*, 4(2):251–257, 1991.  
 404  
 405 Kurt Hornik, Maxwell Stinchcombe, and Halbert White. Multilayer feedforward networks are universal approximators. *Neural networks*, 2(5):359–366, 1989.  
 406  
 407 Diederik P Kingma and Jimmy Ba. Adam: A method for stochastic optimization. *arXiv preprint arXiv:1412.6980*, 2014.  
 408  
 409 Min Lin, Qiang Chen, and Shuicheng Yan. Network in network. *arXiv preprint arXiv:1312.4400*, 2013.  
 410  
 411 Seppo Linnainmaa. Taylor expansion of the accumulated rounding error. *BIT Numerical Mathematics*, 16(2):146–160, 1976.  
 412  
 413 Andrew L Maas, Awni Y Hannun, Andrew Y Ng, et al. Rectifier nonlinearities improve neural network acoustic models. In *Proc. icml*, volume 30, pp. 3. Atlanta, GA, 2013.  
 414  
 415 Diganta Misra. Mish: A self regularized non-monotonic activation function. *arXiv preprint arXiv:1908.08681*, 2019.  
 416  
 417 Vinod Nair and Geoffrey E Hinton. Rectified linear units improve restricted boltzmann machines. In *Proceedings of the 27th international conference on machine learning (ICML-10)*, pp. 807–814, 2010.  
 418  
 419 Prajit Ramachandran, Barret Zoph, and Quoc V Le. Searching for activation functions. *arXiv preprint arXiv:1710.05941*, 2017.  
 420  
 421  
 422  
 423  
 424  
 425  
 426  
 427  
 428  
 429  
 430  
 431 Frank Rosenblatt. The perceptron: a probabilistic model for information storage and organization in the brain. *Psychological review*, 65(6):386, 1958.

- 432 David E Rumelhart, Geoffrey E Hinton, and Ronald J Williams. Learning representations by back-  
433 propagating errors. *Nature*, 323(6088):533–536, 1986.
- 434
- 435 Shibani Santurkar, Dimitris Tsipras, Andrew Ilyas, and Aleksander Madry. How does batch normal-  
436 ization help optimization? *Advances in neural information processing systems*, 31, 2018.
- 437
- 438 Simone Scardapane, Steven Van Vaerenbergh, Simone Totaro, and Aurelio Uncini. Kafnets: Kernel-  
439 based non-parametric activation functions for neural networks. *Neural Networks*, 110:19–32,  
440 2019.
- 441 Paul J Werbos. Applications of advances in nonlinear sensitivity analysis. In *System Modeling*  
442 *and Optimization: Proceedings of the 10th IFIP Conference New York City, USA, August 31–*  
443 *September 4, 1981*, pp. 762–770. Springer, 2005.

## 444

### 445 A AUTHORS STATEMENT ON THE USE OF LARGE LANGUAGE MODELS

### 446 (LLMs)

### 447

448 This work was conducted with the assistance of a large language model (LLM), specifically Gemini,  
449 used as a general-purpose writing and ideation tool. The role of the LLM was significant enough to  
450 warrant disclosure.

451

452 The LLM was used primarily to enhance the clarity, structure, and flow of the manuscript. Its  
453 contributions include:

- 454 • Refining and organizing the text: The model was used to improve sentence structure, gram-  
455 mar, and overall coherence across various sections, including the introduction and conclu-  
456 sions. It helped restructure disorganized ideas into a logical narrative that is easier for  
457 readers to follow.
  - 458 • Improving academic tone: The LLM was prompted to formalize the language and termi-  
459 nology to align with the standards of scientific writing, ensuring that the manuscript’s tone  
460 is professional and precise.
  - 461 • Reviewing and editing: The model was used to review text sections, identify redundancies,  
462 and propose alternative phrasing for conciseness and impact. It also helped to rephrase  
463 specific sentences to more accurately reflect the authors’ intended meaning.
- 464

465 It is important to note that the LLM did not perform any original research, data analysis, or interpret  
466 experimental results. All core ideas, experimental designs, and data interpretations are exclusively  
467 the intellectual property of the authors. The LLM acted just as a sophisticated writing and editing  
468 assistant, similar to how a human co-author might provide feedback on prose and structure.

469

470

471

472

473

474

475

476

477

478

479

480

481

482

483

484

485